

Atomic scale characterization of buried In x Ga 1 - x As quantum dots using pulsed laser atom probe tomography

M. Müller, A. Cerezo, G. D. W. Smith, L. Chang, and S. S. A. Gerstl

Citation: *Applied Physics Letters* **92**, 233115 (2008); doi: 10.1063/1.2918846

View online: <http://dx.doi.org/10.1063/1.2918846>

View Table of Contents: <http://scitation.aip.org/content/aip/journal/apl/92/23?ver=pdfcov>

Published by the [AIP Publishing](#)

Articles you may be interested in

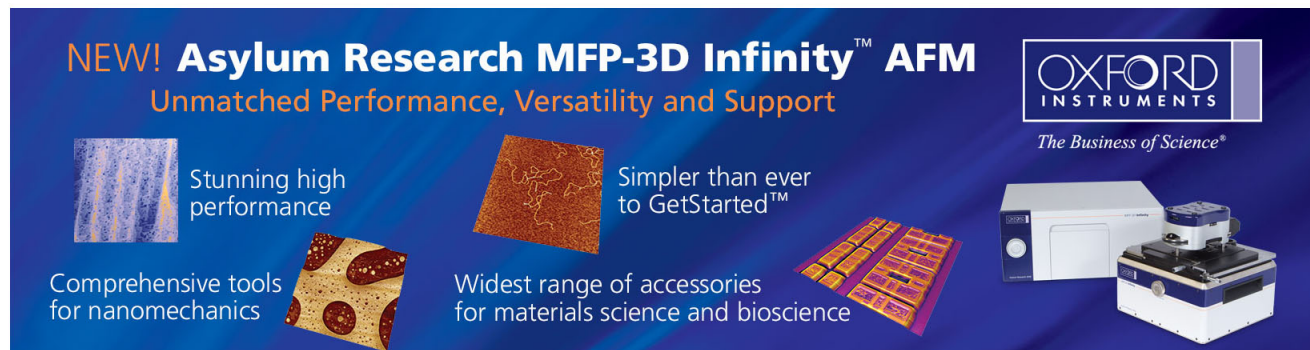
Effects of In x Ga 1 - x As matrix layer on InAs quantum dot formation and their emission wavelength
J. Appl. Phys. **100**, 033109 (2006); 10.1063/1.2220477

Optical properties of low-strained In x Ga 1 - x As Ga As quantum dot structures at the two-dimensional–three-dimensional growth transition
J. Appl. Phys. **100**, 013503 (2006); 10.1063/1.2208296

Long wavelength emitting In As Ga 0.85 In 0.15 N x As 1 - x quantum dots on GaAs substrate
Appl. Phys. Lett. **88**, 231902 (2006); 10.1063/1.2209879

One-dimensional postwetting layer in In Ga As Ga As (100) quantum-dot chains
J. Appl. Phys. **99**, 033705 (2006); 10.1063/1.2169868

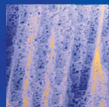
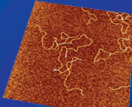
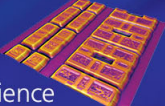
Electroreflectance studies of InAs quantum dots with In x Ga 1 - x As capping layer grown by metalorganic chemical vapor deposition
Appl. Phys. Lett. **86**, 131917 (2005); 10.1063/1.1894613



NEW! Asylum Research MFP-3D Infinity™ AFM
Unmatched Performance, Versatility and Support

OXFORD INSTRUMENTS
The Business of Science®

Stunning high performance
Simpler than ever to GetStarted™
Comprehensive tools for nanomechanics
Widest range of accessories for materials science and bioscience


Atomic scale characterization of buried $\text{In}_x\text{Ga}_{1-x}\text{As}$ quantum dots using pulsed laser atom probe tomography

M. Müller,^{1,a)} A. Cerezo,¹ G. D. W. Smith,¹ L. Chang,² and S. S. A. Gerstl²

¹Department of Materials, University of Oxford, Parks Road, Oxford OX1 3PH, United Kingdom

²Department of Material Science and Engineering, National Chiao Tung University, 1001 Ta Hsueh Road, Hsinchu, Taiwan 300, Republic of China

³Imago Scientific Instruments, 5500 Nobel Drive, Suite 100, Madison, Wisconsin 53711, USA

(Received 26 March 2008; accepted 11 April 2008; published online 13 June 2008)

Atom probe tomography (APT) has been used to study $\text{In}_x\text{Ga}_{1-x}\text{As}$ quantum dots buried in GaAs. The dots have an average base width of 16.1 ± 1.1 nm and height of 3.5 ± 0.3 nm, but a wide range of sizes. APT composition profiles across the dots are similar to a previous study by cross-sectional scanning transmission electron microscopy, but show significant gallium incorporation (average $x = 0.22 \pm 0.01$). The direct three-dimensional nature of the APT data also reveals the complex spatial distribution of indium within the dots. Data such as these are vital for optimizing the performance of quantum dot materials and devices. © 2008 American Institute of Physics.

[DOI: 10.1063/1.2918846]

The physical properties of quantum dot systems depend on many parameters, e.g., chemical composition, morphology, and chemical environment.¹ In order to adjust specific properties, comprehensive nanoscale information about the dots and their surroundings is required. However, the analysis of overgrown quantum dots is challenging. Numerous attempts at analyzing such dots have been published, mainly using either transmission electron microscopy (TEM)^{2–9} or scanning tunneling microscopy.^{10–15} X-ray techniques^{16,17} have also been applied. A major problem is the fact that overgrown quantum dots are hard to observe without uncovering them. Thus, past microscopic studies have mainly focused on cross-sectional investigations. A recent approach aimed at a direct compositional analysis of buried quantum dots using aberration-corrected scanning TEM (STEM).⁹ With a combination of high-angle annular dark-field (HAADF) imaging, electron energy-loss spectroscopy, and computer calculations, it was possible to obtain information about the indium distribution. However, such TEM techniques are still essentially two-dimensional, and assumptions must be made about the three-dimensional (3D) shape of the dots. For example, Wang *et al.*⁹ assumed a faceted quantum dot, in the form of a truncated pyramid, in order to derive composition profiles from their TEM data. The present study shows that pulsed-laser atom probe tomography (APT) uniquely enables direct 3D, high spatial resolution imaging, and chemical analysis of buried InGaAs quantum dots, providing additional insights into these materials.

The material investigated was a quantum dot layer system consisting of 30 pairs of 2.62 ML of InAs overgrown by 30 nm GaAs. This alternating layer system was grown on a GaAs substrate and was capped with 60 nm GaAs and 30 nm AlAs. The growth itself was carried out without interruption using molecular beam epitaxy at base pressures between 2 and 5×10^{-11} Torr. The InAs layers were grown at 485 °C with 0.28 Å/s and the GaAs cap at 600 °C with 3 Å/s using an As₄ source.

APT investigations require sharp needle-shaped tips with a radius of curvature smaller than 100 nm and a small taper angle. For the present study, a dual-beam focused ion beam based lift-out and annular milling procedure was applied using a FEI NanoLab 600 with an *in situ* Omniprobe micromanipulator, at Imago Scientific Instruments, Madison, WI, USA. A lift-out sample was cut out from a flat piece of material perpendicular to the (001) surface.¹⁸ In order to avoid gallium implantation and ion-beam damage, a protective ~60 nm thick nickel layer was sputtered on top of the sample material. Further protection was ensured by deposition of a 100–200 nm thick platinum layer using ion-beam platinum deposition. Moreover, cleanup steps at low ion beam current and acceleration voltage were applied in order to remove ion-beam damaged surface regions.¹⁹

The instrument used for this study was an Imago Scientific Instruments LEAP™ 3000X Si local-electrode atom probe equipped with a diode-pumped Nd:YVO₄ solid-state laser operating at the second harmonic frequency of 532 nm with a pulse duration of <15 ps. Analyses were performed at 20–30 K base specimen temperature, 250 kHz laser pulse repetition frequency, and laser pulse energies of approximately 0.01–0.06 nJ with a laser spot size of ~2–3 μm. These analyses resulted in significant datasets containing tens of millions of ions and crossing up to ten layer pairs. Data were reconstructed using IVAS™ APT software incorporating standard reconstruction algorithms.²⁰

Figure 1 shows a 3D atom map of the quantum-dot material along its growth direction. For a clear representation, only the detected indium atoms are displayed. The quantum dots are represented by small regions of higher indium ion counts located on the wetting layer. Detailed analysis of the data shows the quantum dots have a lens shaped morphology. No clear indication for faceting could be visualized in the 3D APT data representation; however, cross-sectional indium profiles taken through the dots, as in Fig. 2, suggest a truncated pyramidal shape as has been indicated by other studies.²¹ The base lengths range from 11.3 to 30.7 nm along the major axis and from 6.9 to 24.8 nm for the minor axis, with an average base length aspect ratio of $1:1.5 \pm 0.1$. The dot heights range from 1.6 to 6.9 nm and the average dot

^{a)}Electronic mail: michael.mueller@materials.ox.ac.uk.

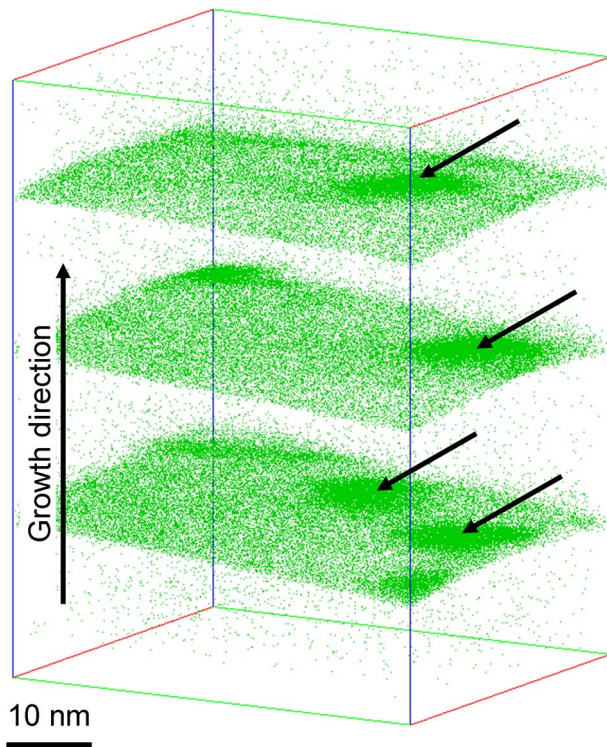


FIG. 1. (Color online) APT atom map showing the indium atoms within three consecutive wetting layers and their associated quantum dots (arrowed). For clarity, the gallium atoms of the capping layers and the arsenic atoms of the wetting and capping layers are not shown. The indium atoms apparent between the wetting layers are considered to be background noise.

height is 3.6 ± 0.3 nm. Individual $\text{In}_x\text{Ga}_{1-x}\text{As}$ quantum dots have compositions in the range of $x=0.11$ - 0.35 , with the mean composition measured as $x=0.22 \pm 0.01$. These variations are critical in controlling the materials properties, since the compositions will affect the InGaAs bandgap, and the size determines the positions of the energy levels within the quantum dot.

Figure 2 shows a two-dimensional indium concentration profile based on a 2 nm thick slice through a representative quantum dot. It should be emphasized that the limited thickness of the slice allows the local compositional fluctuations within the dot to be revealed. The two-dimensional concentration profile shows very clearly the different indium re-

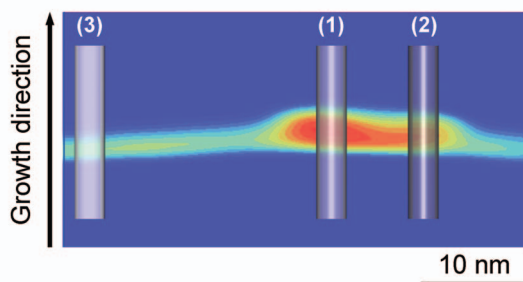
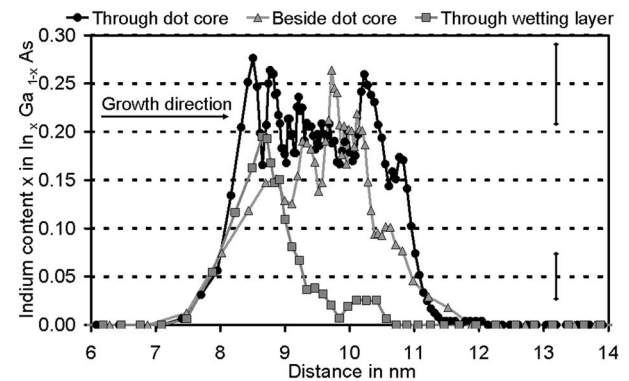
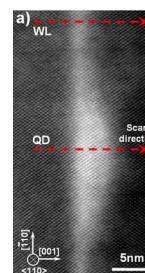


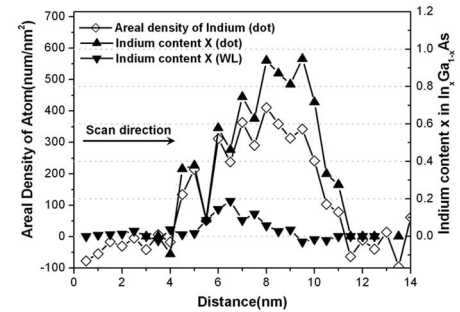
FIG. 2. (Color) Two-dimensional indium concentration profiles obtained from a 2 nm thick slice cut through the center of a quantum dot parallel to the growth direction. The colors are directly related to the indium concentration in the slice, where red implies the highest indium content of $x \sim 0.28$ in $\text{In}_x\text{Ga}_{1-x}\text{As}$ and blue the absence of indium (apart from indium counts caused by background noise). The intersecting cylinders (1), (2), and (3) were used to calculate the one-dimensional indium profiles in Fig. 3(a).



(a)



(b)



(c)

FIG. 3. (Color online) (a) One-dimensional indium composition profiles from the three different regions of the single quantum dot shown in Fig. 2, as indicated by the cylinders: (1) intersecting the indium rich core (\bullet), (2) beside the core (\triangle), and (3) through the wetting layer (\square). Exemplary error bars are given on the left side of the graph for $x=0.05$ and $x=0.25$. [(b) and (c)] Results from the STEM investigations of Wang *et al.* (Ref. 9): (b) HAADF image and (c) corresponding indium composition profile, reprinted with permission.

gions within the quantum dot, consisting of an indium-rich core that is vertically centered but laterally shifted. The shifts seen in different dots are in similar directions within a single layer, and in different directions from one layer to another, suggesting that the observation is a genuine feature of the quantum dots and not an artifact of the data collection and reconstruction procedures used in APT. Cross-sectional TEM work by Lemaître *et al.*⁶ has also suggested lateral indium content variations. It is interesting to note that recent in-depth analysis of the light emission from InGaN epilayers have indicated the presence of complex strain fields associated with the transition from planar to Stranski-Krastanow growth.²² There may be a link between these complex strains and the complexity of composition variations seen in the present work. Santoprete *et al.*²³ have argued, based on an atomistic interdiffusion model that chemical disorder within pyramidal quantum dots significantly reduces the strain field inside the dots.

Figure 3 shows three one-dimensional concentration profiles through a quantum dot and the wetting layer, generated from the 3 nm diameter cylinders shown in Fig. 2. One of them intersects the indium-rich core with the maximum indium content (\bullet -graph). Here, the indium-rich core contains up to $x=0.28 \pm 0.04$ indium in $\text{In}_x\text{Ga}_{1-x}\text{As}$ depending on the actual position of the intersecting cylinder. The spatially averaged indium concentration of this particular dot is $x=0.18 \pm 0.01$. In order to clarify the differences between the quantum dot and the wetting layer, a concentration profile

(-□-graph in Fig. 3) was also calculated through the wetting layer, showing a lower maximum indium concentration here of $x=0.20 \pm 0.04$. A direct comparison with the work of Wang *et al.*⁹ indicates similar concentration profiles for indium (Fig. 3). In contrast, the maximum indium concentration in the dot as concluded from APT investigations is significantly smaller, although that of the wetting layer is comparable. Moreover, no evidence was found for an almost pure InAs region within this dot or any of the large number of others evaluated. This is explained by the higher capping temperature used here, compared to that used for the material studied by Wang *et al.* (480 °C),⁹ which would lead to stronger intermixing of gallium and indium. Although the model does not include capping, kinetic modeling of intermixing during quantum dot formation by Heyn *et al.* has shown that at higher growth temperatures more gallium from the substrate layer is incorporated into the growing dots.²⁴ In their model, choosing a value of 2.3 eV as the activation energy for gallium atoms to jump onto the wetting layer surface gives a quantum dot composition of $x \approx 0.2$ at 600 °C, as seen here, but $x \approx 1$ at 480 °C as seen by Wang *et al.*⁹

APT provides a powerful method for 3D characterization of buried quantum dots. This study has revealed the variability of dot size and shape, the complexity of their chemistry, and the degree of intermixing between the dots/wetting layers and the GaAs capping layers. APT is complementary to other techniques, in particular TEM, but importantly provides direct atomic-scale measurement of the size, shape, and chemistry of the quantum dots without making assumptions about any of these parameters in interpreting the data. Information such as this is vital not only in optimizing the properties of the quantum dot materials, but also for maximizing the reproducibility and reliability of devices.

The UK facility for atomic scale analysis has been established with funding from the Engineering and Physical Sciences Research Council (EPSRC) under Grant No. EP/077664/1. M.M. gratefully acknowledges the EPSRC for funding under Grant No. EP/C540379/1, the “Hamburger Stiftung für Internationale Forschungs- und Studienvorhaben” and the “Studienstiftung des deutschen Volkes” for additional bursaries. M.M. and A.C. also thank Imago Scientific Instruments for funding. The authors are also grateful to Ray O’Neill (Imago) for sample preparation. LEAP and IVAS

are trademarks of Imago Scientific Instruments.

- ¹A. P. Alivisatos, *Science* **271**, 933 (1996).
- ²D. Zhi, H. Davock, R. Murray, C. Roberts, T. S. Jones, D. W. Pashley, P. J. Goodhew, and B. A. Joyce, *J. Appl. Phys.* **89**, 2079 (2001).
- ³P. A. Crozier, M. Catalano, R. Cingolani, and A. Passaseo, *Appl. Phys. Lett.* **79**, 3170 (2001).
- ⁴K. Ozasa, Y. Aoyagi, M. Iwaki, and H. Kurata, *J. Appl. Phys.* **94**, 313 (2003).
- ⁵D. Zhi, M. Wei, R. E. Dunin-Borkowski, P. A. Midgley, D. W. Pashley, T. S. Jones, B. A. Joyce, P. F. Fewster, and P. J. Goodhew, *Microelectron. Eng.* **73-74**, 604 (2004).
- ⁶A. Lemaître, G. Patriarche, and F. Glas, *Appl. Phys. Lett.* **85**, 3717 (2004).
- ⁷A. Sauerwald, T. Kümmell, D. Peskes, G. Bacher, A. Löffler, J. P. Reithmaier, and A. Forchel, *Appl. Phys. Lett.* **89**, 023121 (2006).
- ⁸G. Costantini, A. Rastelli, C. Manzano, P. Acosta-Diaz, R. Songmuang, G. Katsaros, O. G. Schmidt, and K. Kern, *Phys. Rev. Lett.* **96**, 226106 (2006).
- ⁹P. Wang, A. L. Bleloch, M. Falke, P. J. Goodhew, J. Ng, and M. Missous, *Appl. Phys. Lett.* **89**, 072111 (2006).
- ¹⁰B. Lita, R. S. Goldman, J. D. Phillips, and P. K. Bhattacharya, *Appl. Phys. Lett.* **75**, 2797 (1999).
- ¹¹N. Liu, J. Tersoff, O. Baklenov, A. L. Holmes, Jr., and C. K. Shih, *Phys. Rev. Lett.* **84**, 334 (2000).
- ¹²D. M. Bruls, J. W. A. M. Vugs, P. M. Koenraad, H. W. M. Salemink, J. H. Wolter, M. Hopkinson, M. S. Skolnick, F. Long, and S. P. A. Gill, *Appl. Phys. Lett.* **81**, 1708 (2002).
- ¹³Q. Gong, P. Offermans, R. Nötzel, P. M. Koenraad, and J. H. Wolter, *Appl. Phys. Lett.* **85**, 5697 (2004).
- ¹⁴P. Offermans, P. M. Koenraad, R. Nötzel, J. H. Wolter, and K. Pierz, *Appl. Phys. Lett.* **87**, 111903 (2005).
- ¹⁵L. Ouattara, A. Mikkelsen, E. Lundgren, L. Höglund, C. Asplund, and J. Y. Andersson, *J. Appl. Phys.* **100**, 044320 (2006).
- ¹⁶P. F. Fewster, V. Holy, and D. Zhi, *J. Phys. D* **36**, A217(2003).
- ¹⁷M. Sztucki, T. U. Schulli, T. H. Metzger, E. Beham, D. Schuh, and V. Chamard, *Superlattices Microstruct.* **36**, 11 (2004).
- ¹⁸K. Thompson, D. Lawrence, D. J. Larson, J. D. Olson, T. F. Kelly, and B. Gorman, *Ultramicroscopy* **107**, 131 (2007).
- ¹⁹K. Thompson, B. Gorman, D. J. Larson, B. Van Leer, and L. Hong, *Microsc. Microanal.* **12**, 1736 (2006).
- ²⁰M. K. Miller, *Atom Probe Tomography: Analysis at the Atomic Level*, (Kluwer Academic/Plenum, New York, London, 2000), p. 239.
- ²¹L. G. Wang, P. Kratzer, N. Moll, and M. Scheffler, *Phys. Rev. B* **62**, 1897 (2000).
- ²²S. M. De Sousa Pereira, K. P. O’Donnell, and E. J. Da Costa Alves, *Adv. Funct. Mater.* **17**, 37 (2007).
- ²³R. Santoprete, P. Kratzer, M. Scheffler, R. B. Capaz, and B. Koiller, *J. Appl. Phys.* **102**, 023711 (2007).
- ²⁴Ch. Heyn, A. Schramm, T. Kipp, and W. Hansen, *J. Cryst. Growth* **301-302**, 692 (2007).